ScientificScholar®
Knowledge is power
Publisher of Scientific Journals

www.surgicalneurologyint.com

Surgical Neurology International

Editor-in-Chief: Nancy E. Epstein, MD, Clinical Professor of Neurological Surgery, School of Medicine, State U. of NY at Stony Brook.

SNI: Neuroanatomy and Neurophysiology

Editor
Seyed Ali Khonsary, MD
University of California at Los Angeles, Los Angeles, CA, USA

SNI
Open Access

Original Article

Dynamic asymmetry in cerebrospinal fluid pressure: An indicator of regional differences in compliance

Connor J. English, Zachary Taylor, Michael Cramberg, Bruce A. Young

Department of Anatomy, Kirksville College of Osteopathic Medicine, Kirksville, Missouri, United States.

E-mail: Connor J. English - connorjenglish@atsu.edu; Zachary Taylor - sa206666@atsu.edu; Michael Cramberg - mcramberg@atsu.edu; *Bruce A. Young - byoung@atsu.edu

***Corresponding author:**
Bruce A. Young,
Department of Anatomy,
Kirksville College of
Osteopathic Medicine,
Kirksville, Missouri,
United States.

byoung@atsu.edu

Received : 25 April 2023
Accepted : 05 May 2023
Published : 02 June 2023

DOI
10.25259/SNI_365_2023

Quick Response Code:

ABSTRACT

Background: Dural compliance influences the shape and magnitude of the cerebrospinal fluid (CSF) pulsations. In humans, cranial compliance is approximately 2× greater than spinal compliance; the differential has been attributed to the associated vasculature. In alligators, the spinal cord is surrounded by a large venous sinus, which suggests that the spinal compartment may have higher compliance than is found in mammals.

Methods: Pressure catheters were surgically implanted into the cranial and spinal subdural spaces of eight subadult American alligators (*Alligator mississippiensis*). The CSF was propelled through the subdural space by orthostatic gradients and rapid changes in linear acceleration.

Results: CSF pressure recordings taken from the cranial compartment were consistently, and significantly, larger than those taken from the spinal compartment. After the myodural bridge of *Alligator* was surgically released, the asymmetry in CSF pressure was decreased.

Conclusion: Unlike the situation in humans, the spinal compartment of *Alligator* has greater compliance than the cranial compartment, presumably due to the presence of the large spinal venous sinus surrounding the dura. The change in CSF pressures after myodural surgical release supports the hypothesis that the myodural bridge functions, at least in part, to modulate dural compliance and the exchange of CSF between the cranial and spinal compartments.

Keywords: Cerebrospinal fluid, Compliance, Meninges, Myodural bridge, Pressure propagation

INTRODUCTION

Recordings of resting, or anesthetized, human cerebrospinal fluid (CSF) pressures yield a distinctive series of pulsations, driven by the cardiac and ventilatory cycles.[7,37] Previous studies have shown that the amplitude and shape of the CSF pressure pulse are influenced by compliance.[2] Compliance can be defined as the ratio of volume change to pressure change, or as the inverse of stiffness.[26] Dural compliance can be experimentally manipulated using orthostatic gradients or postural changes[1,22] or by "opening" the skull.[2] The most common experimental manipulation is an infusion study, during which set volumes of fluid are introduced into the CSF compartment, changing the total pressure and CSF pressure pulsations.[18,33] A natural manipulation of this system occurs when humans stand erect; the collapse of the jugular drainage changes the hemodynamics, compliance, and CSF pressure within the skull.[16]

The compliance in the mammalian central nervous system (CNS) is not constant. In the skull, the dura is fused to the periosteum, effectively making much of the epidural space a potential one,[10,32] but there is an extensive vascular component including the dural sinuses. Along the spinal cord, the dura is surrounded by a true epidural space containing adipose tissue and vascular elements.[11] Previous studies have shown that the cranial compartment accounts for roughly 70% of the total dural compliance in humans.[26,36] The transition between the cranial and spinal dural systems occurs at the level of the foramen magnum,[8] where the dura frequently supports folds or low bulges that project into the CSF.[17] This same general region of the spinal dura serves as the insertion of skeletal muscle fibers, forming the myodural bridge;[31] previous workers have hypothesized that the myodural bridge could modulate dural compliance.[13]

The present study was conducted on the American alligator (*Alligator mississippiensis*). In the alligator, the spinal cord extends throughout the trunk and the tail,[11] and there is no terminal meningeal cistern as there is in humans [Figure 1a]. The dura of the alligator undergoes a transition at the foramen magnum [Figure 1b], where the dura is contacted by the well-developed myodural bridge in the alligator.[39] The cranial dura of *Alligator* is not fused to the periosteum;[3,21] the spinal dura of *Alligator* is not surrounded by adipose tissue, but by a large venous sinus[42] which fills the majority of the vertebral canal [Figure 1c].

The purpose of this study was to examine how the compliance of the dural complex of *Alligator*, particularly the presence of the surrounding venous blood-filled spinal sinus and the myodural bridge, influenced pressure pulsations in the CSF. Previous studies have explored the functional "exchange" of CSF between the cranial and spinal compartments.[24,27] The present study is based on a novel simple way of inducing bi-directional CSF lability, which was designed to propel the CSF between the cranial and spinal compartments. Ultimately, the goal of the study was to test whether differential compliance within the spinal and cranial compartments of *Alligator* would lead to differential directional lability of the CSF.

MATERIALS AND METHODS

Live animals

Eight subadult (150–187 cm total length) *A. mississippiensis* were obtained from the Louisiana Department of Wildlife and Fisheries. The alligators were housed communally in a 29 m^2 facility that featured three submerging ponds, natural light, and artificial lights on a 12:12 cycle. The facility was maintained at 30–33°C, warm water rain showers were provided every 20 min, which helped maintain the facility at >75% relative humidity. The alligators were maintained on a diet of previously frozen adult rats. The husbandry and use of the live alligators followed all applicable federal guidelines and were approved by the IACUC of A.T. Still University (Protocol #226, approved March 2022).

Basic experimental preparation

When an individual animal was removed from the enclosure, it was caught by noosing, and its jaws taped shut around a bite pad using vinyl tape. The alligator was then placed on a stiff board (244 × 28 × 3.8 cm thick), which exceeded the maximum width and length of the alligators used for this study. Six 2.5 cm wide heavy duty straps (Northwest Tarp and Canvas; Bellingham, WA) were used to secure the alligator to the board; the straps were tight enough to minimize movement of the animal but not tight enough to impede ventilation or circulation.

With the alligator's mouth held open by the bite pad, a laryngoscope was used to depress the gular valve and expose the glottis. A cuffed endotracheal tube was inserted into the larynx and connected to a custom anesthesia system that included a ventilator pump (Harvard), Vaporstick anesthesia machine (Surgivet), isoflurane vaporizer (Surgivet), and Capnomac Ultima respiratory gas monitor (Datex-Engstrom). The alligators were maintained on a steady ventilatory pattern of 6–8 breaths/min (depending on size) each with a tidal volume of 500 mL. Anesthesia was accomplished using 5% isoflurane. The alligator's EKGs were recorded using two silver chloride surface cup electrodes (019-477200, GRASS, Natus Medical, Pleasanton, CA), coated with a layer of conducting gel (Signagel, Parker Laboratories, Fairfield, NJ), and placed on the ventral surface of the animal on either side of the heart. The electrodes were connected to a P511 preamplifier (GRASS).

A stainless steel surgical burr was used to bore an approximately 4 mm diameter portal through the sagittal midline of the skull just caudal to the orbits. This allowed for direct exposure of the dura mater; a small incision in the dura was used to inset a segment of polyethylene (PE) tubing into the subarachnoid space. A laminectomy was performed at the equivalent of the L2 level to expose the venous sinus [Figure 1d]. A pressure catheter was inserted, and venous blood pressure recorded. Then, a dorsal incision was made in the venous sinus and a surgical portal to the dura constructed using hemostatic powder (Surgicel, Ethicon). This approach permitted the placing of a pressure catheter within the spinal CSF without obstructing blood flow through the venous sinus, or exposing the pressure catheter to the venous blood.

The pressure catheters were connected to P23AA fluid pressure transducers (Statham), which were filled with reptilian Ringer's solution. The pressure transducers were mounted to the board at a fixed site immediately adjacent

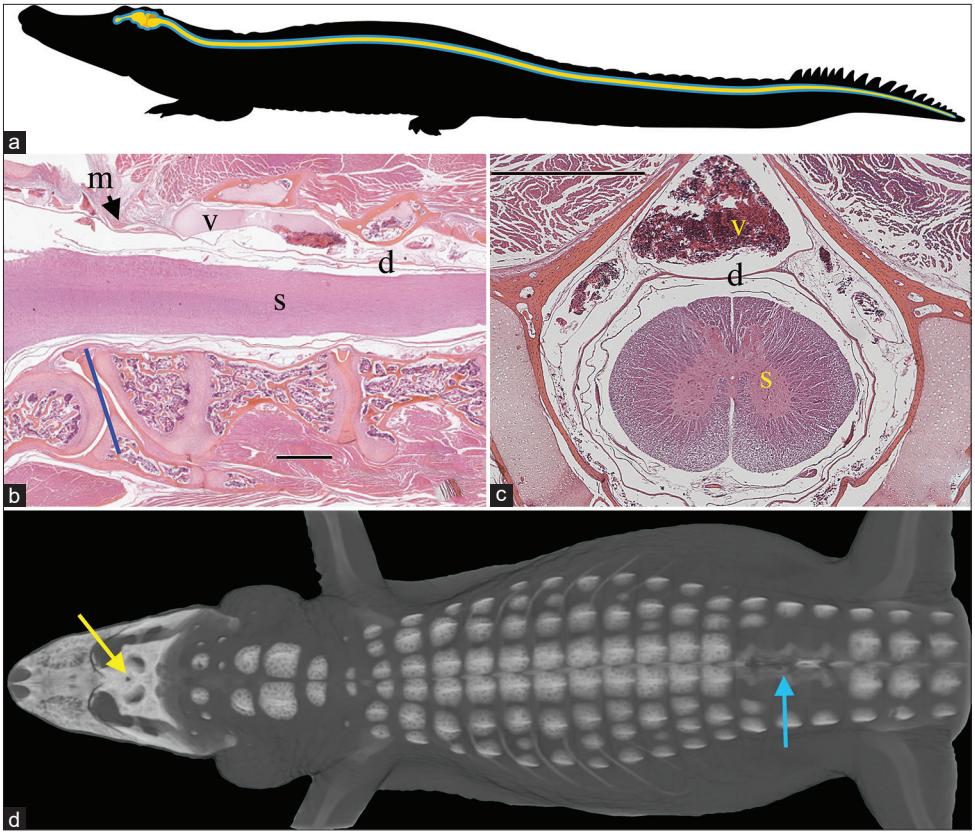

Figure 1: Spinal anatomy of *Alligator mississippiensis*. (a) Schematic of the central nervous system (yellow) and surrounding cerebrospinal fluid (CSF)-filled subdural space (blue); the spinal cord extends to the tip of the tail. (b) Sagittal section through the foramen magnum (blue line) showing the spinal cord (s), dura (d), and the surrounding spinal venous sinus (v). As the dura transitions from the cranial to spinal configuration, it is contacted by the skeletal muscle fibers of the myodural bridge (m). The black line is cited as the scale bar (c) Transverse section through the cervical spinal region showing the spinal venous sinus (v) around the dura (d) and spinal cord (s). (d) Surgical approach illustrated on a 3-D reconstruction of CT data from a 172 cm alligator. The small surgical opening in the skull (yellow arrow) was used to record the cranial CSF pressure, while a laminectomy was performed (blue arrow) to allow for recordings of spinal venous blood pressure and spinal CSF pressure. Scale bars in b and c are both 1 mm.

to, and level with, the surgical exposures, so that rotation of the alligator did not produce a pressure head between the PE tubing and the transducer. The implantation of the PE tubing was snug enough that no CSF leakage was observed; yet, the functionality of the coupling was evident by the (pressure-driven) movement of the CSF along a distance of the catheter. The pressure transducers were coupled to P122 preamplifiers (GRASS). The cranial and spinal pressure catheters were separated by a mean of 51.6 cm. This experimental preparation resulted in stable baseline CSF pressure waves that reflected a combination of ventilatory (at ~0.18 Hz) and cardiac (at ~0.33 Hz) influences [Figure 2].

The CSF pressures, EKG, and ventilatory pattern (from the exhalatory gas analyzer) were recorded simultaneously (at 4.0 kHz) using the MiDas data acquisition system (Xcitex). The CSF pressure transducers were individually calibrated following each experiment. The recorded signals were quantified using the MiDas software, then exported for power spectral analysis using SpectraPlus (Pioneer Hill Software).

Propelling the CSF

Once a stable surgical baseline had been established, two different methods were used to generate experimental pulses in the CSF. After the implantation of the spinal venous or CSF pressure catheter, the alligator was exposed to an orthostatic gradient by rotating the preparation 30° head-up or head-down. The axis of rotation was located approximately 3 cm caudal to the spinal pressure catheter; in all preparations, the cranial and spinal pressure catheters were on the same side of the pivot point for rotation.

Following the orthostatic trials, the surgical board the alligator was strapped to was placed onto a cart with casters resting in a track. The transducers were anchored to the

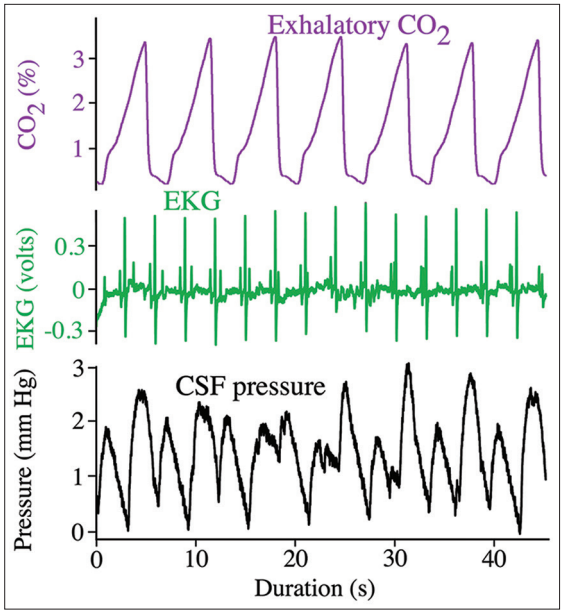

Figure 2: Simultaneous recordings of the ventilatory cycle (top trace, purple), cardiac cycle (middle trace, green), and cranial cerebrospinal fluid (CSF) pressure (bottom trace, black) from *Alligator mississippiensis*. Note that the CSF pressure contains pulsations linked to both the cardiac and ventilatory cycles.

surgical board, so their position relative to the alligator or the pressure catheter did not change. The pressure catheter itself was buttressed between the surgical incision and the transducer so that it was not impinged on, but all displacement was prevented. The cart supporting the anesthetized alligator was then quickly accelerated forward or backward over a distance of approximately 30 cm, then abruptly stopped. The acceleration and stopping was performed manually, this, combined with occasional contact between the casters and the track, meant that the push-pull curves were not always perfectly smooth [Figure 3]. Four accelerations were performed in both directions; with a minimum baseline period of 10 s between each acceleration. For each push/pull trial, the differential in CSF pressure between the baseline and the peak in the first direction of pressure change was quantified (hereafter termed "peak" pressure), this pressure corresponded to the initial period of acceleration. This peak pressure was always followed by a rapid shift in pressure (of sufficient magnitude to change the sign of the pressure); the difference between these two pressure peaks is herein termed the "total pressure" [Figure 3].

The displacements of the alligator were recorded using digital video cameras (Action Camera, YI Technology). The visual records were imported into Kinovea (kinovea.org), the instantaneous velocities were determined and combined with the mass of the alligator to yield momentum.

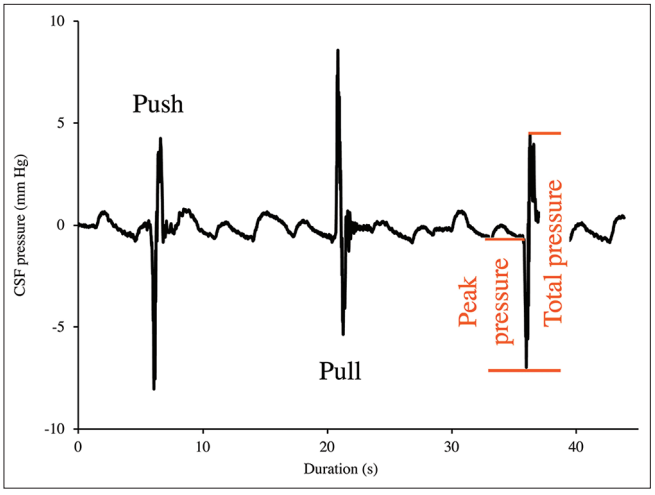

Figure 3: Cranial cerebrospinal fluid (CSF) pressure from three consecutive "push-pull" trials. The push trials result in an initial decrease in cranial CSF pressure, followed by a larger pressure increase; the pull trials result in an initial increase in cranial CSF pressure followed by a larger pressure decrease. For all the trials, the amplitude of the initial spike was defined as "peak pressure" while the amplitude of the following (larger) spike was defined as "total pressure."

Myodural release

After a full set of data were collected, a surgical myodural release was performed. The goal of this release was to disrupt all the tendinous attachments to the dura on both the rostral and caudal sides of the atlas, without disrupting the structural integrity of the spinal dura itself. An additional round of push/pull trials was performed following the myodural release.

RESULTS

Orthostatic gradients

The orthostatic gradients produced consistent results, in part, because there was no evidence of a compensatory mechanism. Three key results [Figure 4] were obtained from the orthostatic trials: (1) the spinal and cranial CSF pressures always shifted in opposite directions; (2) the head-up and head-down rotations resulted in similar magnitudes of change in spinal venous blood and spinal CSF pressure; and (3) the magnitude of change in cranial CSF pressure produced by head-down rotation was roughly 150% that resulting from head-up rotation [Figure 4]. Multivariate analysis of variance (MANOVA) of the cranial pressures during the orthostatic trials found significant (F = 10.91, P = 0.0004) differences among the pressures; Tukey's *post hoc* analyses revealed that the differences were between head-down and head-up postures, and between the cranial CSF and the other pressures.

If the pressure heads [Figure 4] generated by the tilting experiments are geometrically resolved, the values for the

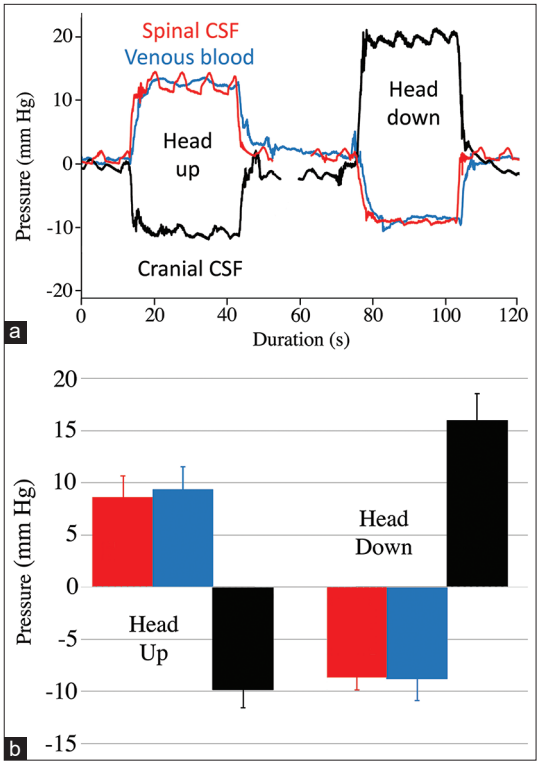

Figure 4: Results from the orthostatic trials. (a) Composite raw data traces recorded from the same 158 cm *Alligator mississippiensis*. The spinal cerebrospinal fluid (CSF) pressure (red line) and venous blood pressure (blue line) exhibit a response similar in magnitude and direction; while the cranial CSF pressure (black line) responds in the opposite direction. The cranial CSF pressure is asymmetric showing a greater response to head-down rotations than to head-up rotations. (b) Graph of the orthostatic results; the height of the bars is the pooled mean for all of the trials, while the error bar represents one standard deviation. The spinal CSF pressure (red) and spinal venous pressure (blue) values were not significantly different; the cranial CSF pressures (black) were significantly different even after rectification.

spinal CSF pressures and the head-up cranial CSF pressure converge on a point corresponding to the heart's location in the trunk of the alligator [Figure 5]. By contrast, the pressure head associated with the cranial CSF head-down trials resolves to a point closer to the actual axis of rotation.

Push/pull experiments

When the cart was accelerated forward (pushed) the CSF pressure increased in the spinal region while decreasing in the cranial region; stopping the cart resulted in a negative spike in spinal CSF pressure and a positive spike in cranial CSF pressure [Figure 6a]. The pattern was exactly opposite when the cart and alligator were accelerated backward, or

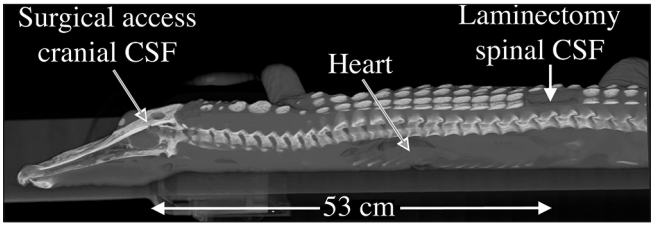

Figure 5: Sagittal DICOM slice through a 172 cm alligator. The mean pressure changes observed during the orthostatic trials were used to calculate the hydrostatic indifference point for *Alligator*; the point resolves to near the caudal margin of the heart.

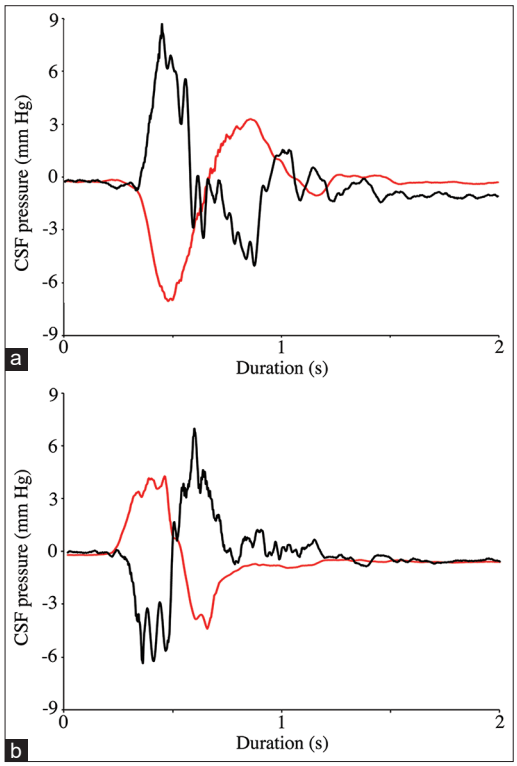

Figure 6: Raw data traces from two consecutive push-pull trials. Note that whether the alligator is pulled (a) or pushed (b) the cranial cerebrospinal fluid (CSF) pressure (black line) and spinal CSF pressure (red line) respond in opposite directions. The amplitude of the cranial CSF pressure changes (both peak and total) was significantly greater than those from the spinal CSF pressure.

pulled, [Figure 6b and Table 1]. The pressure traces shown in Figure 6 (which are successive trials from the same alligator) illustrate three consistent findings: (1) the pressure changes in the cranial and spinal regions were not identical; (2) within both regions, the relationship between the peak and total pressures was not constant; and (3) the cranial pressure traces revealed pulsations after the "total pressure" spike (herein termed "secondary pulses") of greater amplitude and number than the secondary pulses recorded from the spinal

CSF. When the peak to total pressure changes are plotted for both regions (cranial and spinal), and both the push and pull data sets [Figure 7], the asymmetry is clear.

MANOVA of the rectified peak pressures [Table 1] yielded significant differences ($F = 23.66$; $P = 1.944 \times 10^{-14}$). *Post hoc* Tukey's analysis found that the two cranial pressures were of the same magnitude, but the spinal pressures were significantly smaller and different from each other. MANOVA of the rectified total pressures [Table 1] also found significant differences among the four data sets ($F = 31.22$; $P = 5.196 \times 10^{-14}$). *Post hoc* Tukey's analysis found that the two cranial pressures were of the same magnitude, but the spinal pressures were significantly smaller and different from each other.

Table 1: The push/pull trials were pooled across 6 alligators to get the following CSF pressure values.

	Push	Pull
Cranial		
Peak	−7.19, 2.04	9.02, 1.63
Total	13.69, 2.67	−14.56, 1.91
Spinal		
Peak	5.07, 1.28	−6.44, 1.59
Total	−7.90, 2.89	11.01, 2.92

CSF: Cerebrospinal fluid. The pressures are expressed in mm Hg, and presented as mean, standard deviation.

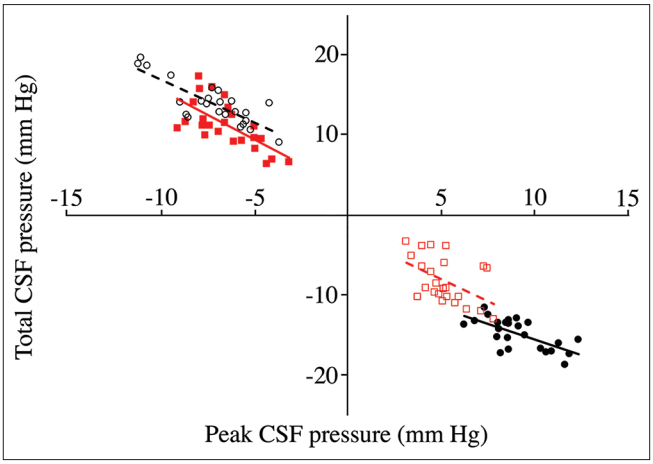

Figure 7: Relation of peak cerebrospinal fluid (CSF) pressure (X-axis) to total CSF pressure (Y-axis) from pooled trials. Data groups are presented as follows: cranial pulls (solid black circles, solid line); cranial push (open black circles, dashed line); spinal pulls (solid red squares, solid line); and spinal push (open red squares, dotted line). As expected, the direction of change in CSF pressure is always opposite in the cranial and spinal regions, opposite in the different directions of displacement, and opposite between peak and total. The cranial CSF pressures recorded during pulls have a different relationship between peak and total pressure than the other three data sets.

The peak instantaneous velocity determined from the video analysis of the push/pull trials was multiplied by the mass of each animal to get momentum (in Newton-seconds, Ns). The pull trials had a pooled mean momentum of 22 Ns (standard deviation, s.d. = 6.2) while the push trials had a pooled mean of 18.97 Ns (s.d. = 6.4). A *t*-test revealed that the momentums present during the two trials were not significantly different ($t = 1.68$, $P = 0.099$).

When the peak [Figure 8a] or total [Figure 8b] CSF pressures are plotted against momentum, the cranial CSF pressures are greater than the spinal CSF pressures (regardless of direction of displacement), and the cranial pressures have a greater regression against momentum than the spinal pressures [Figure 8]. The influence of the momentum was reduced/removed by zeroing the slopes of the regression lines. When the momentum-adjusted peak CSF pressures from the cranial site are plotted against those recorded from the spinal region [Figure 8c], for any given cranial CSF peak pressure, the corresponding spinal CSF peak pressure was significantly greater during the rearward (pull) displacements than during the forward (push) displacements ($t = 9.122$, $P < 0.00001$). Similarly, if the momentum-adjusted data are plotted with total CSF pressure during rearward displacement, against total CSF pressure during forward displacement [Figure 8d], the cranial pressures were significantly greater ($t = 4.084$, $P = 0.00018$).

Secondary pulses

Secondary pulses in the CSF were observed following all of the experimental manipulations [Figures 6 and 9]. The amplitude of these secondary pulses in the spinal CSF (mean = 1.2 mm Hg, s.d. = 0.37) was not significantly different ($t = 1.67$, $P = 0.114$) from the amplitude in the cranial CSF (mean = 1.4 mm Hg, s.d. = 0.68). The fundamental frequencies of the cranial (mean = 7.04 Hz, s.d. = 2.58) and spinal (mean = 7.1 Hz, s.d. = 1.1) secondary pulses were not significantly different ($t = 0.1366$, $P = 0.8921$).

Myodural release

The myodural release had no significant influence on the peak pressures, nor any of the pressures produced by pulling the alligator backward [Table 2]. The myodural release did result in a significant increase in total CSF pressure recorded at both the spinal ($t = 2.29$, $P = 0.032$) and cranial ($t = 2.31$, $P = 0.043$) sites during the "pull" trials [Table 2]. Secondary pulses recorded after the surgical myodural release [Figures 8 and 9] had significantly lower amplitudes ($F = 18.82$, $P < 0.00001$) and fundamental frequencies ($F = 20.99$, $P < 0.0000023$) than either the cranial or spinal pre-release secondary pulses.

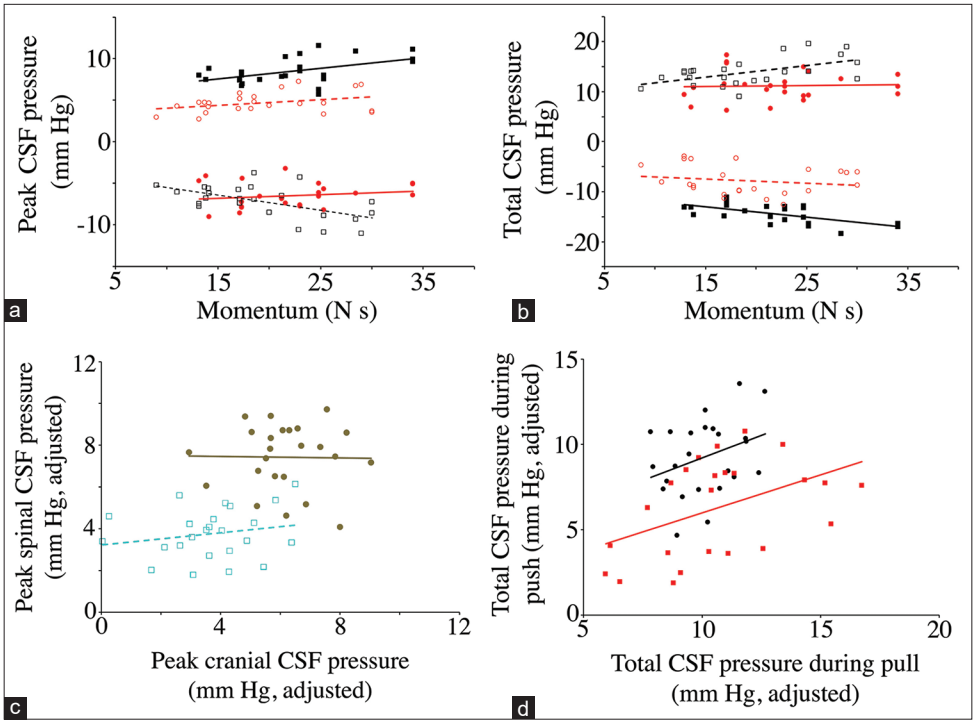

Figure 8: Dynamic asymmetry in the push-pull data. The relationship between momentum and peak (a) and total (b) cerebrospinal fluid (CSF) pressure. Data groups are presented as follows: cranial pulls (solid black squares, solid line); cranial push (open black squares, dotted line); spinal pulls (solid red circles, solid line); and spinal push (open red circle, dashed line). As expected, the direction of change in CSF pressure is always opposite in the cranial and spinal regions, and opposite in the different directions of displacement. Note that the cranial values are larger than the spinal values, and that the regression lines for the cranial data have larger slopes than do those for the spinal data. (c) Relation of peak CSF pressure measured in the skull (X-axis) to peak CSF pressure measured along the spinal cord (Y-axis). These data have been adjusted to eliminate the variation attributable to momentum. Rearward displacement (pull) is indicated by solid brown markers, forward displacement (push) is indicated by open light blue markers. Note that pulling the animal produced greater CSF pressures, particularly in the spinal region. (d) Relation of total CSF pressure measured during rearward displacement (X-axis) to total CSF pressure measured during forward displacement (Y-axis). These data have been adjusted to eliminate the variation attributable to momentum. Cranial data are black circles, spinal data are red squares. Note that the cranial CSF pressures are generally greater than those measured from the spinal cord, though both data sets have a similar regression relationship.

DISCUSSION

Due to the relatively closed nature of the CSF and venous systems, and the integrity of the vertebrate heart, orthostatic gradients in vertebrates resolve around the hydrostatic indifference point of the body, not the axis of rotation.[14] In humans,[25] other mammals[19] and in the present study [Figure 5], the hydrostatic indifference point lies close to the heart. In vertical humans, the concept of a hydrostatic indifferent point is contentious since the collapse of the jugular vein alters the physics of the system.[34] In the present study, the head-up tilts were pressure balanced; the blood pressure in the spinal venous sinus rose slightly above the CSF pressure effectively compensating for the loss of cranial CSF pressure [Figure 4]. Similar compensatory offsets between CSF and venous pressure form the functional coupling between ventilatory intrathoracic pressures and CSF motility in humans.[9]

If a compensatory system is functioning during the head-down rotations, it is not as effective. While the spinal pressure and spinal venous blood pressure changes are symmetrical, the increase in cranial CSF pressure observed during head-down rotation is significantly greater than the decrease in pressure with head-up rotation [Figure 4]. The net increase in cranial pressure causes papillary edema, increase in the optic nerve diameter, and a significant increase in the diameter of the jugular vein.[20,21] Presumably, the differential increase in cranial pressure reflects a pooling of venous (and possibly arterial?) blood, but that pooling does not result in a differential loss of venous pressure at the spinal sinus.

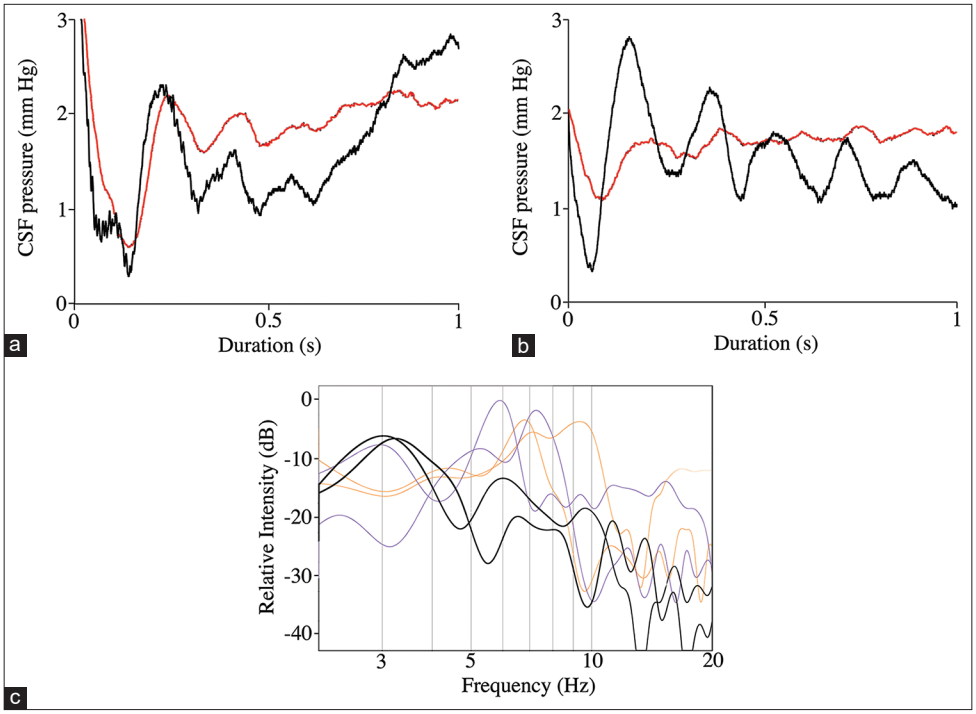

Figure 9: Secondary pulses associated with the push-pull trials. (a) Representative data trace showing the cranial (black line) and spinal (red line) pressure pulses recorded immediately after the total pressure curve. The curves were rectified to facilitate viewing, but are otherwise raw data. Note the close temporal and amplitude patterns of the spinal and cranial secondary cerebrospinal fluid (CSF) pulses. (b) Representative data trace showing the cranial (black line) and spinal (red line) pressure pulses recorded immediately after the total pressure curve. The curves were rectified to facilitate viewing, but are otherwise raw data. These data traces were recorded after the surgical myodural release. Note that after release, the spinal CSF secondary pulses have a significantly lower amplitude and a lower fundamental frequency. (c) Power spectral analysis of the secondary pulses. The spinal and cranial CSF secondary pulses recorded before myodural release (thin lines) are not significantly different and have mean fundamental frequencies near 7 Hz; the spinal CSF secondary pulses (thick lines) recorded after myodural release has significantly lower fundamental frequencies (near 3 Hz).

The push/pull experiments were designed to create an impulse acting on the CSF. The preparation was first accelerated in one direction; the inertia of the CSF caused it to accumulate opposite the direction of the acceleration (causing differential "peak" readings at the two CSF pressure sensors). When the preparation was then rapidly stopped, the resulting impulse caused the CSF to flow opposite the initial movement (causing a reversal in both CSF pressure sensors, the "total" values, which were always greater than the initial peak pressures). Inertial shifts in the CNS are a well-known source of neural trauma.[28,29] Inertial shifts in the CSF of humans have been shown in conjunction with rotation of the head;[38] and recent work has shown a link between natural body movements and CSF pressure dynamics.[40,41]

The push/pull trials consistently yielded asymmetric results; the pressure change in the cranial compartment was significantly greater than the pressure change in the spinal compartment [Table 1]. This differential cannot be explained by differential momentum. The significant difference between cranial and spinal pressures is present whether the data are examined with respect to momentum [Figure 8a and b] or independent of momentum [Figure 8c and d]. Trials in which the preparation was initially accelerated backward (or "pulled") produced significantly greater changes in CSF pressure, even though the momenta generated were not significantly different than those used during the "push" trials [Figure 8c].

Both the orthostatic gradient and push/pull experiments yielded asymmetric results in which cranial CSF pressures and/or cranial CSF pressure changes were significantly greater than spinal CSF pressures. We hypothesize that the dynamic asymmetry results from differential compliance. Previous experimental studies in humans have used the introduction of extra fluids (infusion studies) or surgical openings in the system to manipulate the compliance of the dura.[2,6] Using these, and other techniques, workers have

Table 2: Pooled mean values for CSF pressure (in mm Hg) recorded immediately before, then immediately following, myodural release surgery.

	Pre myodural release			
	Cranial		Spinal	
	Peak	Total	Peak	Total
Pull	9.1	−15.88	−6.51	13.09
Push	−7.83	12.81	6.76	−9.16
	Post myodural release			
	Cranial		Spinal	
	Peak	Total	Peak	Total
Pull	9.64	−16.03	−7.35	13.52
Push	−7.08	**14.96**	6.76	**−12.39**

CSF: Cerebrospinal fluid. Pressures that changed significantly are indicated in bold type

shown that the cranial compliance is roughly 2× the spinal compliance in humans.[26] Our results suggest a very different balance of compliance in *Alligator*; assuming equal volumes of CSF were displaced during the push/pull trials (there was no significant difference in momentum between the two directions), the pressures shown in Table 1 suggest that of the total compliance, the spinal compartment contributes 58% and the cranial compartment 42%. The balance of compliance in *Alligator* is nearly opposite what is seen in humans and other mammals. Presumably, this reflects the large venous sinus located around the spinal dura; as has been previously noted,[26] it is the vasculature that ultimately determines most of the compliance, the large spinal venous sinus leads to a large spinal compliance.

The relationship between spinal and cranial dural compliance in *Alligator* is likely more variable than it is in humans, due to the presence of the large spinal venous sinus in *Alligator* [Figure 1c]. If *Alligator* can actively control blood pressure within the spinal venous sinus, it could actively modulate the spinal dural compliance and, potentially, the dynamics of the CSF between the cranial and spinal compartments. Since these experiments were performed under isoflurane anesthesia, any active venous regulation would have been eliminated. The pressure recordings taken from the spinal venous sinus clearly indicate that the venous pressure is dynamic and functionally tied to spinal CSF pressure [Figure 4]. Bruner[4] described an unusual sphincter in the venous drainage of the crocodilian skull; this sphincter, the presence of which has never been confirmed, would produce a simple mechanism for the regulation of spinal venous pressure.

There are (at least) three important limitations to this study. This study examined only CSF pressure, not CSF flow. Herein, it is assumed that the cranial and spinal CSF was equally influenced by the orthostatic gradients and push/pull trials. It takes some 3500 mm Hg of pressure to induce cavitation in CSF;[5] the external forces applied to the anesthetized alligators during the push/pull trials were not sufficient to render the CSF into discrete cranial and spinal volumes. The second limitation is that the present study did not document direct exchange (absorption or secretion) between the CSF and the vascular system. Such exchange is well-known from infusion studies.[18] The orthostatic gradients were maintained for 30 s during which there was no evidence of shifting CSF pressure levels [Figure 4], and the push/pull manipulations had a short enough time span [typical <0.5 s, Figure 6] that vascular "compensation" was likely minimal. The third limitation was the use of a single spinal recording site. The spinal CSF pressure was recorded from a point roughly mid-way along the length of the spinal cord of *Alligator* [Figure 1]. The pressure waves recorded at this point do not appear to have been attenuated by the more rostral portions of the spinal cord (as was described in humans[36]), but without cervical spinal pressure recordings we could not assess that empirically.

Regardless of which experimental means was used to produce the pulses of CSF pressure, the pulses were consistently followed by "secondary pulses." These secondary pulses were of much lower amplitude [Figures 6 and 9] than the experimental pressure pulses. The secondary pulses had a mean fundamental frequency of 7 Hz, which is higher than the cardiac or ventilatory CSF pulsation frequencies (0.33 and 0.18 Hz, respectively). Herein, the secondary pulsations are interpreted as "harmonic" pulsations produced by the experimental pressure pulse propagating along the length of the alligator's CNS. In this interpretation, the primary influence on the physical properties of these harmonic pulses would be the physical properties of the CNS (i.e., length of the subdural space), these were constant regardless of the different methods used to generate the experimental pulses. The amplitude of these harmonic pulses is low enough that the differential dural compliance is unlikely to have had a significant impact; these pulses are the only ones analyzed in the present study that did not show a significant difference between cranial and spinal pressures. Similar harmonics have been described from studies of CSF pressure in humans[15,36] and have been used to assess compliance of neural tissue.[30]

The myodural bridge of *Alligator* is well-developed, and contraction of the myodural bridge changes the CSF pressure.[39] There continues to be debate regarding the functional role and significance of the myodural bridge;[12,23] two common hypotheses are that the myodural bridge functions to alter CSF pressure, or that it adjusts/regulates the dura.[13] The results of the present study support both these hypotheses; more specifically, our data suggest that the myodural bridge of *Alligator* is functioning to regulate the

transition in dural compliance at the foramen magnum and that, by doing so, it plays a role in influencing the dynamics of CSF exchange between the cranial and spinal compartments. In these experiments, surgical disruption of the myodural bridge increased the bulk flow of CSF out of the spinal compartment (presumably by dilating the rostral portion of the spinal dura) and increased the propagation time of the secondary pulsations (presumably by creating localized turbulence at the foramen magnum). A recent contribution[35] examined how pathological conditions within the myodural bridge could alter compliance of structures around the foramen magnum in mice. Our conclusion is similar, but we would argue that the relationship between the myodural bridge, dural compliance, and CSF pressure is a regular part of the CSF dynamics influencing the flow and pressure of the CSF in both the healthy and pathological states.

CONCLUSION

External forces, applied as gravitational gradients or linear accelerations, resulted in differential pressure changes in the cranial and spinal (CSF). Herein the induced differential changes in CSF pressure are interpreted as reflecting differential compliance within the cranial and spinal compartments. The results suggest that in Alligator, the spinal compartment has higher dural compliance than the cranial compartment (which is opposite the situation found in humans); the spinal dural compliance of Alligator is likely determined by the presence of a large spinal venous sinus. Differential blood pressure within the spinal sinus, like differential activation of the myodural bridge, has the potential to modulate the compliance of the spinal compartment and influence CSF exchange between the brain and spinal cord.

Acknowledgements

The authors wish to thank the Louisiana Department of Wildlife and Fisheries who kindly provided the alligators used in this study, and P. Kondrashov for his continued support of this research program. Figure 1a was skillfully rendered by Jamie Carroll.

Declaration of patient consent

Patient's consent not required as there are no patients in this study.

Financial support and sponsorship

Nil.

Conflicts of interest

There are no conflicts of interest.

REFERENCES

1. Alperin N, Hushek SG, Lee SH, Sivaramakrishnan A, Lichtor T. MRI study of cerebral blood flow and CSF flow dynamics in an upright posture: The effect of posture on the intracranial compliance and pressure. Acta Neurochir Suppl 2005;95:177-81.
2. Anile C, Bonis PD, Ficola A, Santini P, Mangiola A. An experimental study on artificially induced CSF pulse waveform morphological modifications. Neurol Res 2011;33:1072-82.
3. Ariens Kappers C. The meninges in lower vertebrates compared with those in mammals. Arch Neurol Psychiatry 1926;15:281-96.
4. Bruner HL. On the cephalic veins and sinuses of reptiles: With description of a mechanism for raising the venous blood-pressure in the head. Am J Anat 1907;7:1-117.
5. Bustamante MC, Cronin DS. Cavitation threshold evaluation of porcine cerebrospinal fluid using a Polymeric Split Hopkinson Pressure Bar-Confinement chamber apparatus. J Mech Behav Biomed Mater 2019;100:103400.
6. Charlton JD, Johnson RN, Pederson NE, Mann JD. Assessment of cerebrospinal fluid compliance and outflow resistance: Analysis of steady-state response to sinusoidal input. Ann Biomed Eng 1983;11:551-61.
7. Czosnyka M, Pickard JD. Monitoring and interpretation of intracranial pressure. J Neurol Neurosurg Psychiatry 2004;75:813-821.
8. de Oliveira E, Rhoton AL Jr., Peace D. Microsurgical anatomy of the region of the foramen magnum. Surg Neurol 1985;24:293-352.
9. Dreha-Kulaczewski S, Joseph AA, Merboldt KD, Ludwig HC, Gärtner J, Frahm J. Identification of the upward movement of human CSF *in vivo* and its relation to the brain venous system. J Neurosci 2017;37:2395-402.
10. Fyneface-Ogan S. Anatomy and clinical importance of the epidural space. In: Epidural Analgesia-Current Views and Approaches. Vol. 12. London, UK: Intechopen; 2012. p. 1-12.
11. Greer S, Cramberg MJ, Young BA. Morphometrics of the spinal cord and surrounding structures in *Alligator mississippiensis*. Biology (Basel) 2022;11:514.
12. Grondel B, Cramberg M, Greer S, Young BA. The morphology of the suboccipital region in snakes, and the anatomical and functional diversity of the Myodural bridge. J Morphol 2022;283:123-33.
13. Hack GD, Koritzer RT, Robinson WL, Hallgren RC, Greenman PE. Anatomic relation between the rectus capitis posterior minor muscle and the dura mater. Spine (Phila Pa 1976) 1995;20:2484-6.
14. Hinghofer-Szalkay H. Gravity, the hydrostatic indifference concept and the cardiovascular system. Eur J Appl Physiol 2011;111:163-74.
15. Holm S, Eide PK. The frequency domain versus time domain methods for processing of intracranial pressure (ICP) signals. Med Eng Phys 2008;30:164-70.
16. Holmlund P, Johansson E, Qvarlander S, Wåhlin A, Ambarki K, Koskinen LD, *et al*. Human jugular vein collapse in the upright posture: Implications for postural intracranial pressure regulation. Fluids Barriers CNS 2017;14:17.

17. Ito K, Yamada M, Horiuchi T, Hongo K. Microanatomy of the dura mater at the craniovertebral junction and spinal region for safe and effective surgical treatment. J Neurosurg Spine 2020;33:165-71.
18. Kasprowicz M, Lalou DA, Czosnyka M, Garnett M, Czosnyka Z. Intracranial pressure, its components and cerebrospinal fluid pressure-volume compensation. Acta Neurol Scand 2016;134:168-80.
19. Klarica M, Kuzman T, Jurjević I, Radoš M, Tvrdeić A, Orešković D. The effect of body position on intraocular and intracranial pressure in rabbits. Acta Neurochir Suppl 2016;122:279-82.
20. Knoche L, Young BA, Kondrashova T. The influence of gravitational gradients on the American alligator (*Alligator mississippiensis*). Anat Physiol Curr Res 2019;9:318.
21. Kondrashova T, Blanchard J, Knoche L, Potter J, Young BA. Intracranial pressure in the American alligator (*Alligator mississippiensis*): Reptilian meninges and orthostatic gradients. J Comp Physiol A Neuroethol Sens Neural Behav Physiol 2020;206:45-54.
22. Kramer LA, Hasan KM, Sargsyan AE, Marshall-Goebel K, Rittweger J, Donoviel D, *et al*. Quantitative MRI volumetry, diffusivity, cerebrovascular flow, and cranial hydrodynamics during head-down tilt and hypercapnia: The SPACECOT study. J Appl Physiol (1985) 2017;122:1155-66.
23. Lai HX, Gong J, Hack GD, Song TW, Liu B, Yu SB, *et al*. Development, maturation, and growth of the myodural bridge within the posterior atlanto-axial interspace in the rat. J Morphol 2022;283:993-1002.
24. Linninger AA, Tangen K, Hsu CY, Frim D, Cerebrospinal fluid mechanics and its coupling to cerebrovascular dynamics. Ann Rev Fluid Mech 2016;48:219-57.
25. Magnaes B. Body position and cerebrospinal fluid pressure. Part 2: Clinical studies on orthostatic pressure and the hydrostatic indifferent point. J Neurosurg 1976;44:698-705.
26. Marmarou A, Shulman K, LaMorgese J. Compartmental analysis of compliance and outflow resistance of the cerebrospinal fluid system. J Neurosurg 1975;43:523-34.
27. Matsumae M, Kuroda K, Yatsushiro S, Hirayama A, Hayashi N, Takizawa K, *et al*. Changing the currently held concept of cerebrospinal fluid dynamics based on shared findings of cerebrospinal fluid motion in the cranial cavity using various types of magnetic resonance imaging techniques. Neurol Med Chir (Tokyo) 2019;59:133-46.
28. McAllister TW. Neurobiological consequences of traumatic brain injury. Dialogues Clin Neurosci 2011;13:287-300.
29. Namjoshi DR, Good C, Cheng WH, Panenka W, Richards D, Cripton PA, *et al*. Towards clinical management of traumatic brain injury: A review of models and mechanisms from a biomechanical perspective. Dis Model Mech 2013;6:1325-38.
30. Nitta M, Kasuga Y, Hasegawa Y, Nagai H. Conduction time of the pulse through the brain with increased intracranial pressure In: Intracranial Pressure. Vol. 5. Berlin: Springer; 1983. p. 211-5.
31. Palomeque-Del-Cerro L, Arráez-Aybar LA, Rodríguez-Blanco C, Guzmán-García R, Menendez-Aparicio M, Oliva-Pascual-Vaca Á. A systematic review of the soft-tissue connections between neck muscles and dura mater: The myodural bridge. Spine (Phila Pa 1976) 2017;42:49-54.
32. Pearcy Q, Jeejo M, Scholze M, Tomlinson J, Dressler J, Zhang M, *et al*. Biomechanics of vascular areas of the human cranial dura mater. J Mech Behav Biomed Mater 2022;125:104866.
33. Qvarlander S, Malm J, Eklund A. CSF dynamic analysis of a predictive pulsatility-based infusion test for normal pressure hydrocephalus. Med Biol Eng Comput 2014;52:75-85.
34. Qvarlander S, Sundström N, Malm J, Eklund A. Postural effects on intracranial pressure: Modeling and clinical evaluation. J Appl Physiol (1985) 2013;115:1474-80.
35. Song X, Gong J, Yu SB, Yang H, Song Y, Zhang XH, *et al*. The relationship between compensatory hyperplasia of the myodural bridge complex and reduced compliance of the various structures within the cranio-cervical junction. Anat Rec (Hoboken) 2023;306:401-8.
36. Takizawa H, Gabra-Sanders T, Miller JD. Changes in the cerebrospinal fluid pulse wave spectrum associated with raised intracranial pressure. Neurosurgery 1987;20:355-61.
37. Wagshul ME, Eide PK, Madsen JR. The pulsating brain: A review of experimental and clinical studies of intracranial pulsatility. Fluids Barriers CNS 2011;8:5.
38. Xu Q, Yu SB, Zheng N, Yuan XY, Chi YY, Liu C, *et al*. Head movement, an important contributor to human cerebrospinal fluid circulation. Sci Rep 2016;6:31787.
39. Young BA, Adams J, Beary JM, Mardal KA, Schneider R, Kondrashova T. The myodural bridge of the American alligator (*Alligator mississippiensis*) alters CSF flow. J Exp Biol 2020;223:jeb230896.
40. Young BA, Cramberg MJ. Treadmill locomotion in the American alligator (*Alligator mississippiensis*) produces dynamic changes in intracranial cerebrospinal fluid pressure. Sci Rep 2022;12:11826.
41. Young BA, Cramberg M. The influence of movement on the cerebrospinal fluid pressure of the American alligator (*Alligator mississippiensis*). Biology (Basel) 2022;11:1702.
42. Zippel KC, Lillywhite HB, Mladinich CR. Anatomy of the crocodilian spinal vein. J Morphol 2003;258:327-35.

How to cite this article: English CJ, Taylor Z, Cramberg M, Young BA. Dynamic asymmetry in cerebrospinal fluid pressure: An indicator of regional differences in compliance. Surg Neurol Int 2023;14:187.